Hindawi
Shock and Vibration
Volume 2023, Article ID 3925252, 12 pages
https://doi.org/10.1155/2023/3925252

Research Article

Study on the Numerical Relationship between Dynamic Compressive Strength and Crushing Energy Consumption in Dynamic Point Load Test under Different Corrosion Conditions

Ming Zhou, Lan Qiao, An Luo, and Qingwen Li

University of Science & Technology Beijing, Beijing 100083, China

Correspondence should be addressed to Qingwen Li; qingwenli@ustb.edu.cn

Received 6 October 2023; Revised 22 November 2023; Accepted 28 November 2023; Published 7 December 2023

Academic Editor: Xiuquan Liu

Compared with most dynamic tests, point load test is widely used in engineering practice because of its wide requirements for test conditions. In offshore mining engineering, the surrounding rock is affected by dynamic load impact and corrosion of various aqueous solutions for a long time. Therefore, it is of great significance to study the influence of hydrochemical corrosion on dynamic mechanical properties of rock to ensure the stability of surrounding rock. In this paper, a large number of dynamic point load and dynamic uniaxial compression tests were carried out on the granite mined from a large mine by using the Split Hopkinson pressure bar test device after the corrosion of pH values of 2, 5, and 7 solutions, respectively. Based on the energy theory, the crushing energy consumption in the test process is analyzed, and finally the fitting formula of the dynamic compressive strength and the crushing energy consumption in the dynamic point load test is obtained through fitting analysis. The results show that when the crushing energy consumption in the dynamic point load test is used to estimate the dynamic compressive strength, a certain crushing energy consumption (the final value of this test is 70 J in this paper) is more accurate, and it can estimate the dynamic compressive strength under various corrosion conditions under this crushing energy consumption. However, with the change of crushing energy consumption in the dynamic point load test, this transformation relationship is no longer accurate, and it is necessary to modify this transformation relationship with corrosion condition as the influencing factor. This conclusion can provide reference for obtaining the dynamic compressive strength of rocks under different corrosion conditions in engineering field in the future.

1. Introduction

Dynamic point load test is a simple method to test the dynamic tensile and compressive properties of rock and other materials under the impact of dynamic point load. Because the requirements of the test conditions and the shape of the test material are much lower than those of dynamic impact compression, dynamic splitting, and other related tests, it has a wider applicability.

At present, many scholars' studies on point load strength mostly focus on static point load, including the relationship between point load strength and uniaxial compressive strength [1–6] and determination of correction coefficient [7–11], while there are few studies on dynamic point load strength. In previous studies, the author [12] has given the transformation relationship between the dynamic point load strength and the corresponding dynamic compressive strength, which lays a foundation for this paper to analyze the change of the transformation relationship between the two after hydrochemical corrosion. On the other hand, from the surface strata to the deep earth, most geological processes and surrounding rock environment changes of underground rock mass are affected by groundwater, and long-term hydrochemical corrosion will greatly change the mechanical properties of rocks, which has become one of the main problems faced by researchers in rock mechanics and engineering at present [13–19]. Karfakis and Akram [20] studied the effect of chemical solution on rock fracture toughness. Heggheim et al. [21] studied the weakening mechanism of seawater on the mechanical properties of

limestone. These studies [22–26] analyzed the laws of influence of different hydrochemical environments on rocks and some even established mathematical relationships between the rate of dissolution, diffusion and precipitation of particles and the stress, and geometrical parameters of cracks and fluid properties. These studies provided theoretical basis for the analysis of the transformation relationship between dynamic point load strength and dynamic compressive strength after corrosion. In summary, it is of great significance to study the changing law of the transformation relationship between dynamic point load strength and dynamic compressive strength under different corrosion conditions.

In this paper, taking granite as the research object, the dynamic impact compression test and dynamic point load test were carried out on the samples before and after corrosion, respectively, and the crushing energy consumption of the samples in the above process was analyzed. Because the dynamic point load test cannot accurately calculate the strain rate, the impact velocity is taken as the intermediate variable to determine the proportional relationship between the crushing energy consumption during the dynamic point load test and the dynamic compression test. At the same time, by changing the pH value of the corrosion solution to accelerate the corrosion, the conversion relationship between the dynamic point load strength and the dynamic compressive strength of the samples with different corrosion degrees was fitted. Finally, the effect of corrosion degree on the conversion relationship is analyzed.

2. Sample Preparation and Test Scheme

2.1. Instrument and Control Method. The dynamic uniaxial compression test adopts Split Hopkinson pressure bar (as shown in Figure 1). The diameter of the pressure rod is 50 mm, its elastic modulus E is 210 GPa, the density is 7787 kg/m^3, the wave velocity is 5667 m/s, and the length of the steel rod is 1.5 m. In Figure 1, we annotated the incident bar (which is also a reflection bar) and the transmission bar and marked the propagation direction of the wave in the bar.

The experimental device of dynamic point load impact test is improved by imitating the loading cone of the static point load test, and the improvement method adds a punch protection sleeve at the impact end of the traditional Hopkinson impact device, as shown in Figure 2.

2.2. Water-Chemical Corrosion Test and Analysis of Rock. Standard samples of Φ50 mm × 25 mm were prepared, and the samples were immersed in acidic salt solution with pH = 2, pH = 5, and pH = 7, respectively, for 60 days. After the samples were corroded to the planned time, they were impacted by different air pressures (corresponding to different incident velocities and different strain rates). In order to reduce the influence of nonuniformity on the test results, all the samples in the test were obtained by cutting a complete granite block with no visible cracks. Part of the samples and the corrosion process are shown in Figure 3.

Figure 1: Split Hopkinson pressure bar test device.

Figure 2: Dynamic point load test bar and sample installation.

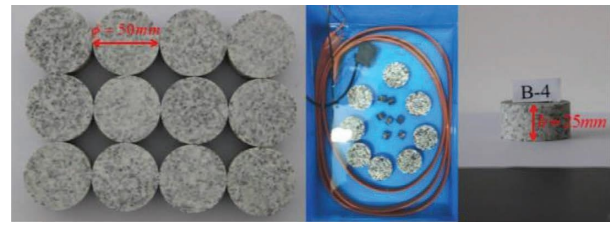

Figure 3: Test specimen and corrosion process diagram.

In order to quantitatively describe the damage degree of corroded rocks, the longitudinal wave velocity of all corroded rocks is measured. The longitudinal wave velocity of rock materials is related to many factors such as mineral particle density, particle size, matrix content, degree of cementation, and pore structure. In order to prevent the accidental measurement of wave velocity and the nonuniformity of corrosion, three measurement methods were adopted to measure the wave velocity: contralateral measurement, ipsilateral measurement, and oblique contralateral measurement. Finally, the average value of the measured wave velocity was taken for analysis. The electron microscope scanning of typical samples corroded by a solution with pH = 2 and pH = 7 is shown in Figure 4. As can be seen from Figure 4, compared with the sample corroded by pH = 7 solution, the surface morphology of the sample corroded by pH = 2 solution showed obvious corrosion traces. The tight structure between different particles became more loose and broken, the intact cementation surface was corroded, and a large number of secondary pores and loose particles appeared, which were the main reasons for the decrease of wave velocity. The longitudinal wave velocity curve of the specimen with time after different hydrochemical corrosions is shown in Figure 5.

It can be observed from Figure 5 that the *P*-wave velocity of all samples decreased after corrosion of different pH solutions. If linear fitting is adopted, the *P*-wave velocity decline slopes of corroded samples with pH values of 2, 5, and 7 are −11.65, −8.78, and −2.07, respectively; that is, the

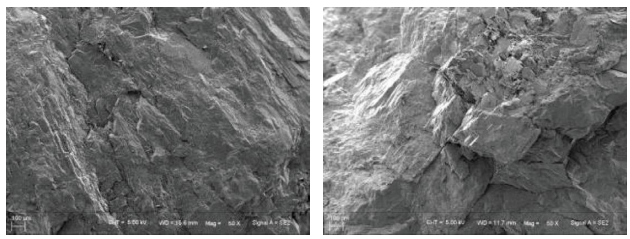

Figure 4: pH = 2 and pH = 7 after salt solution soaking of 60 d under scanning electron microscopy of granite sample.

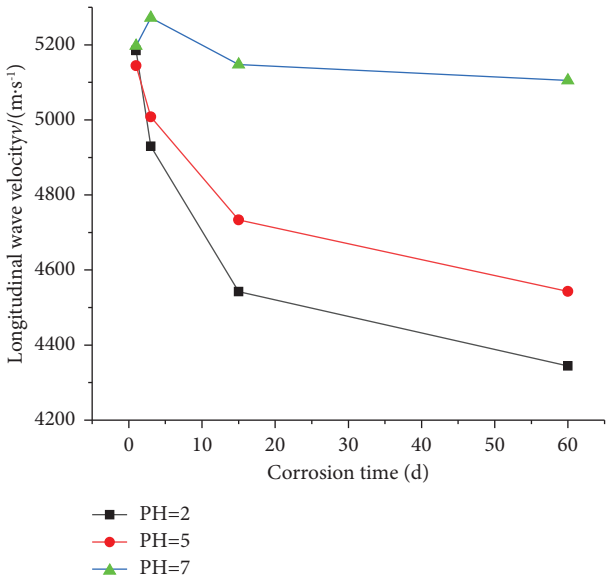

Figure 5: Curve of longitudinal wave velocity change with time after corrosion with different solutions.

lower the pH value, the faster the wave velocity declines and the greater the final change range. At the same time, it can be observed that the change rate of wave velocity is large in the initial stage of the experiment and tends to be gentle in the later stage. It is worth noting that in the solution with pH = 7, although the longitudinal wave velocity of the sample remains basically unchanged in general, there is a small increase in the early stage. This is because in the early stage of corrosion, ions in the salt solution precipitate and adhere to the pores on the rock surface. Since the corrosion rate of granite in the neutral solution is very slow, the rate of wave velocity reduction caused by corrosion is lower than the rate of wave velocity increase caused by ion precipitation in the solution, resulting in an increasing trend of the curve in the early stage of the test.

3. Test Results and Analysis

3.1. Analysis of Energy Conversion during the Dynamic Compression Test. Since the dynamic compression test satisfies the one-dimensional stress state and the assumption of stress-strain uniformity, we can obtain the stress, strain, and strain rate of the impact rock by using the three-wave formula.

At the same time, we can obtain the incident energy, reflected energy, transmitted energy, and crushing absorption energy of rocks in the process of impact compression and failure through the energy formula, as shown in the following formulas:

$$W_i = \frac{A_0 C_0}{E} \int \sigma_i^2 \mathrm{d}t = A_0 C_0 E \int_0^t \varepsilon_i^2 \mathrm{d}t, \quad (1)$$

$$W_r = \frac{A_0 C_0}{E} \int \sigma_r^2 \mathrm{d}t = A_0 C_0 E \int_0^t \varepsilon_r^2 \mathrm{d}t, \quad (2)$$

$$W_t = \frac{A_0 C_0}{E} \int \sigma_t^2 \mathrm{d}t = A_0 C_0 E \int_0^t \varepsilon_t^2 \mathrm{d}t, \quad (3)$$

$$W_a = W_i - W_r - W_t, \quad (4)$$

where W_i is the incident energy; W_r is the reflection energy; W_t is the transmission energy; and W_a is the energy consumption of the broken. A_0 is the cross-sectional area of the bar; C_0 is the propagation velocity of stress wave in the bar; E is the elastic modulus of the pressure bar; σ_i, ε_i are the stress and strain parameters of the incident bar; σ_r, ε_r are the stress and strain parameters of the reflecting bar; and σ_t, ε_t are the stress and strain parameters of the transmission bar.

According to the three-wave formula and the energy formula, the impact velocity, incident energy, and crushing energy of the sample corroded by the pH = 7 solution during the test were statistically analyzed. It should be noted that since the dynamic point load test described above cannot effectively calculate the dynamic strain rate, we use the impact velocity instead of the strain rate as the intermediate medium to deduce the final conversion relationship. The stress-strain curves of the samples corroded by pH = 7 solution under different impact velocities are shown in Figure 6.

As can be seen from Figure 6, both dynamic elastic modulus and peak stress of granite exhibit obvious strain rate effects with the increase of strain rate and both the dynamic elastic modulus and peak stress show an increasing trend.

Table 1 shows the statistical table of impact velocity, dynamic compressive strength, and various energies during the impact compression test of the sample corroded by a pH = 7 solution. The energy time-history curves of some typical impact compression tests are shown in Figure 7.

It can be seen from the figure that with the increase of impact velocity, the incident energy of granite increases and the crushing energy consumption also increases. The relationship between crushing energy consumption and impact velocity of the sample during the impact compression failure process was fitted, as shown in Figure 8(a). The fitting formula is $W_1 = 11.372v - 70.963$, and the coefficient of determination R^2 is 0.99, indicating a good degree of fitting. The crushing energy consumption of the impact compression test is fitted with the corresponding dynamic uniaxial compressive strength, as shown in Figure 8(b). The fitting formula is $W_1 = 0.337\sigma - 5.07$, and the coefficient of determination R^2 is 0.99. The models had high fitting degree.

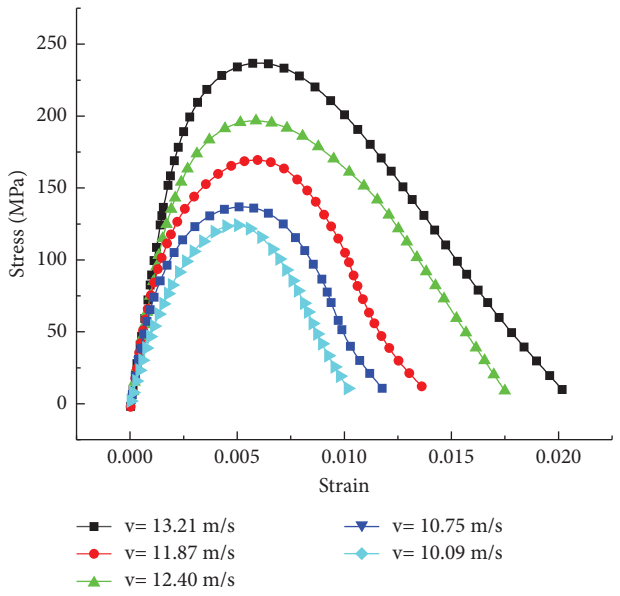

Figure 6: Dynamic compressive stress-strain curves of rocks corroded with pH = 7 solution at different impact velocities.

Table 1: Statistical table of test data on impact compression of samples after corrosion of PH = 7 solution.

Sample number	V (m·s^{-1})	W_i (J)	σ (MPa)	W (J)
1	9.67	93.12	117.34	40.65
2	10.09	95.16	125.35	42.33
3	10.75	113.62	151.26	51.69
4	11.87	138.24	174.09	62.17
5	12.40	154.47	192.14	70.23
6	13.21	167.62	242.13	80.31

Similarly, we did the same treatment on the corroded samples with the solution with pH = 2 and pH = 5, and the changing laws of different mechanical strength characteristics of rocks were analyzed under the same impact velocity (same strain rate). It is worth noting that the impact pressure can only be strictly controlled during the impact process, but the impact speed generated by the same impact pressure is not exactly the same, which also results in little difference between the data of the corroded solution with pH = 7 and the dry noncorroded sample, because the impact of a slight difference in impact velocity counteracts the impact of slight corrosion.

In order to ensure the effectiveness of the comparison of test data, we conducted multiple sets of experiments here and tried to select experimental groups with similar impact velocities in the three solutions for comparison. Figure 9 shows the dynamic compressive stress-strain curves of rocks corroded by different corrosion solutions at the impact velocity of 12.74 m/s. It can be seen from the figure that after chemical corrosion, the peak stress of the sample has a certain degree of damage, and the stronger the acidity of the solution, the more severe the corrosion and greater the strength reduction, and the proportion of the compacted part in the rising part of the stress-strain curve is significantly increased. At the same time, the ductility of the stress-strain curve is prominent after the peak point. We also made statistics on the impact velocity, dynamic compressive strength, and various energies of corroded samples with the solution with pH = 2 and pH = 5 during the impact compression experiment, as shown in Table 2. The relationship between crushing energy consumption, impact velocity, and dynamic compressive strength in two cases was fitted, respectively, and the results are shown in Figures 10 and 11.

It can be seen from Table 2 that with the decrease of pH value of corrosion solution; that is, with the increase of corrosion degree, the dynamic uniaxial strength decreases at the same impact speed and the crushing energy consumption in the process of impact compression decreases. That is to say, more energy is converted to the elastic energy of the compaction stage. At the same time, we can also observe that with the increase of impact velocity; that is, with the increase of strain rate, the corroded specimens still show obvious rate effect.

As can be seen from Figure 12, as the pH value of the solution decreases, that is, the degree of corrosion increases, the dynamic compressive strength value of the sample after corrosion gradually decreases, and the downward trend is consistent regardless of the impact speed.

It can be seen from Figures 10 and 11 that the crushing energy consumed by corroded specimens in the impact compression crushing test still maintains a good linear relationship with the impact velocity and the dynamic compressive uniaxial strength. We fit the linear relationship between the two cases, respectively, and the results are as follows: The fitting relationship between the crushing energy consumption of the sample corroded by salt solution with pH = 2 and the impact velocity is $W_1 = 11.696v - 76.003$, and the coefficient of determination R^2 is 0.98, indicating a good degree of fitting. The fitting relationship between crushing energy consumption and the corresponding dynamic uniaxial compressive strength is as follows: $W_1 = 0.411\sigma - 8.476$, coefficient of determination R^2 is 0.96, and the models had high fitting degree. The fitting relationship between crushing energy consumption and impact velocity of the sample corroded by salt solution with pH = 5 is $W_1 = 11.518v - 78.427$, and the coefficient of determination R^2 is 0.99, indicating a good degree of fitting. The fitting relationship between crushing energy consumption and the corresponding dynamic uniaxial compressive strength is as follows: $W_1 = 0.406\sigma - 8.347$, coefficient of determination R^2 is 0.98, and the fitting degree is good.

3.2. Analysis of Energy Conversion during Dynamic Point Load Test before and after Corrosion. Because the dynamic point load test improved the punch of the test instrument, the whole test device no longer satisfied the basic assumption of the three-wave formula during the test. Therefore, we cannot use the three-wave formula to calculate the stress-strain curve and strain rate during the test. However, the strain collected on the incident bar (reflection bar) and transmission bar on the test instrument is directly collected by the strain gauge data, which do not involve the three-wave

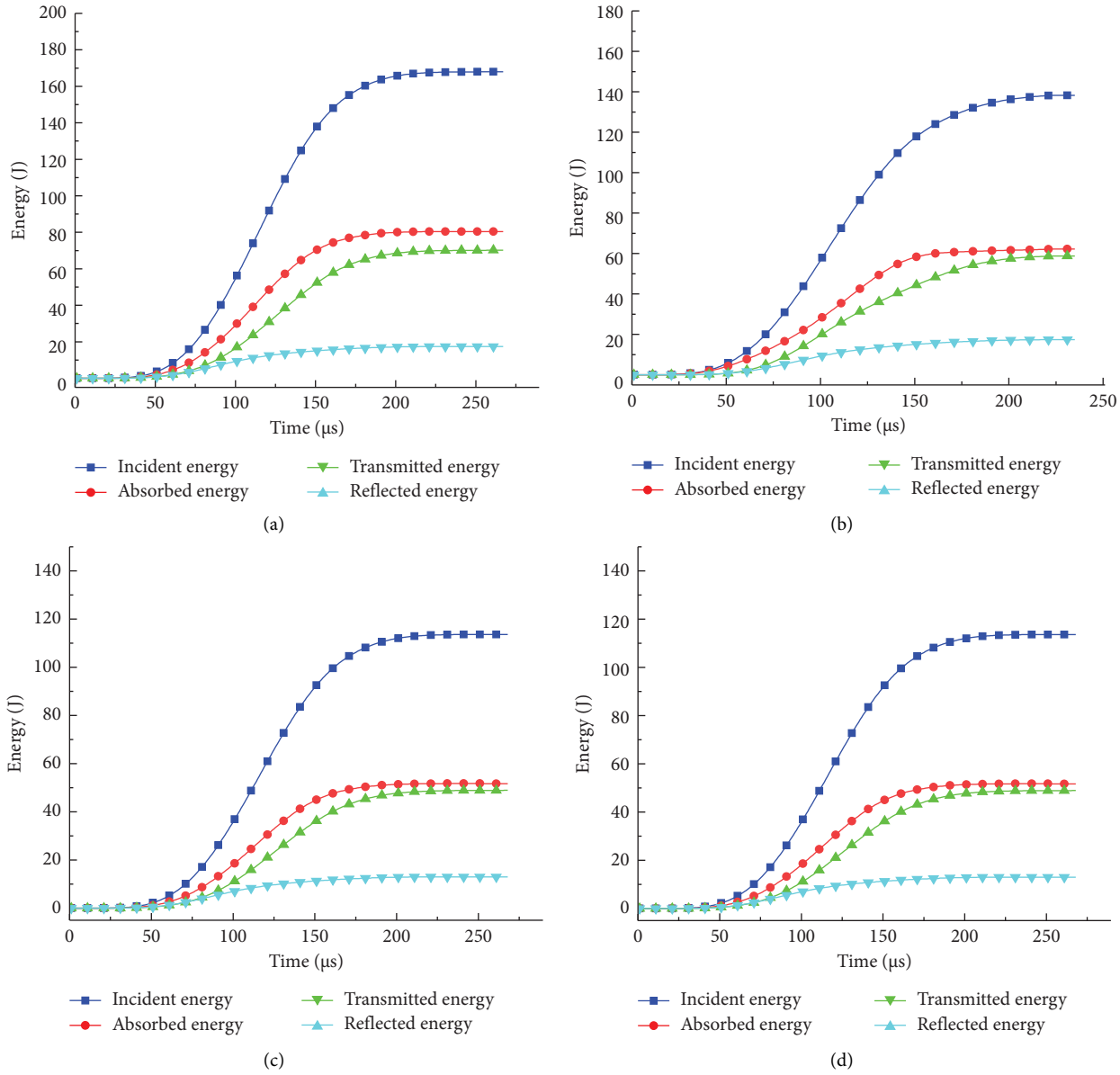

Figure 7: The energy time history of part of the impact compression test of the sample corroded by the solution with pH = 7: (a) impact velocity of 13.21 m/s, (b) impact velocity of 11.87 m/s, (c) impact velocity of 10.75 m/s, and (d) impact velocity of 9.67 m/s.

formula. Therefore, based on the energy formula, we can take the impact velocity as the intermediate medium to analyze the whole dynamic point load impact process and take the energy as the reference object to compare and analyze with the dynamic compression test. It should be noted that in the dynamic point load test conducted in this paper, the punch cone angle is selected as 60°, which is because at present, the cone angle is selected as 60° in the static point load test. The influence law of the cone angle on the point load strength before and after corrosion will be further analyzed in the future research. Figures 13 and 14, respectively, show the energy time-history curves of the dynamic point load tests under different impact velocities after solution corrosion with partial pH = 2 and pH = 7 (pH = 5 is not listed).

As can be seen from the analysis of Figures 13 and 14, compared with the impact compression test, the reflected energy of the dynamic point load test is almost 0, and the transmitted energy increases. For the same impact velocity, when the incident energy hardly changes, more energy is converted into crushing energy consumption in the process of impact damage. When the impact velocity is the same, with the decrease of pH value of corrosion solution (the increase of corrosion degree), both the incident energy and crushing energy consumption tend to decrease. This is because corrosion reduces the brittleness and improves the ductility, and there is a trend of conversion from brittleness to ductility, so the crushing energy consumption becomes lower. The impact velocity, incident energy, and crushing energy consumption of the impact point load test after

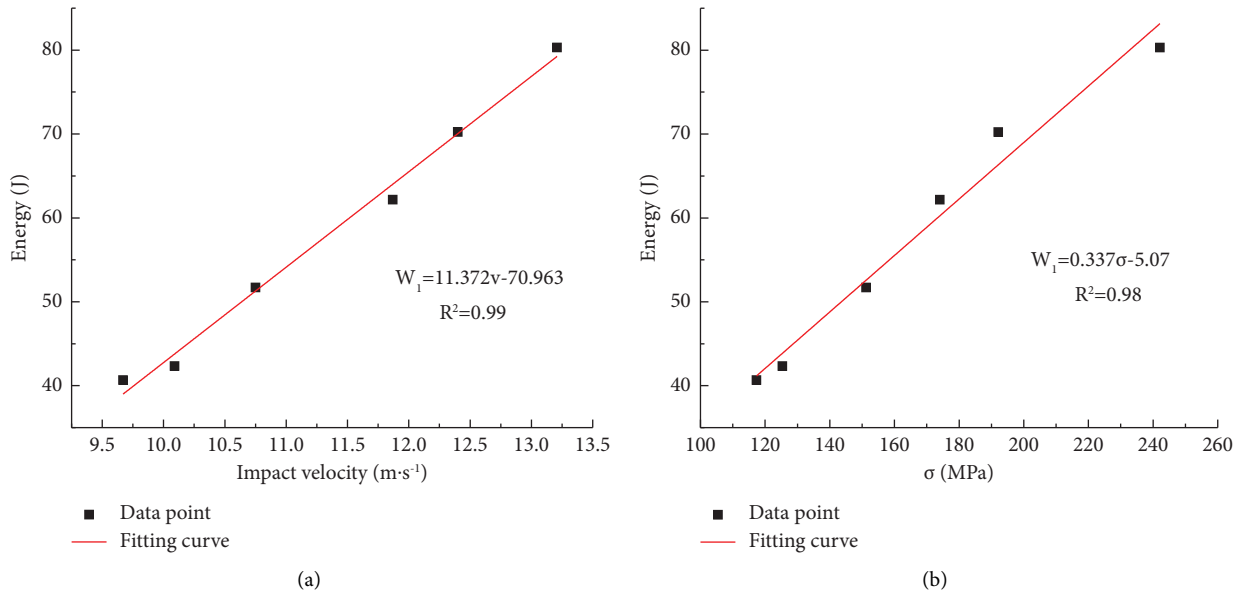

Figure 8: The fitting relationship between crushing energy consumption and impact velocity and dynamic compressive strength in the impact compression experiment of pH = 7 solution after corrosion: (a) impact velocity-crushing energy consumption fitting curve and (b) dynamic compressive strength-crushing energy consumption fitting curve.

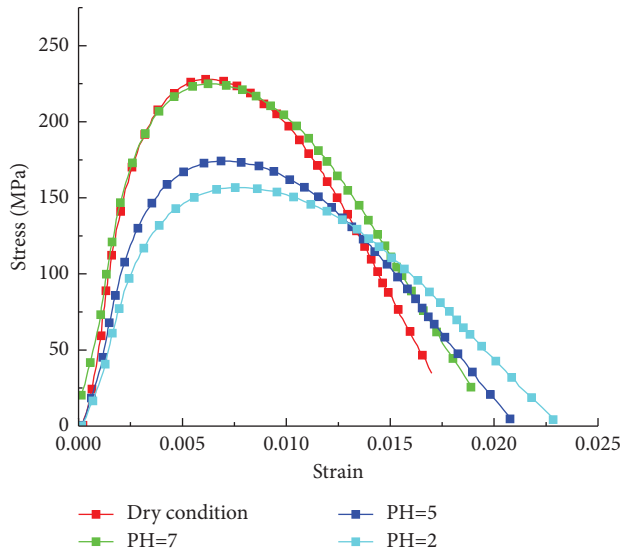

Figure 9: Dynamic compressive stress-strain curves of rocks corroded with pH = 7 solution at same impact velocities.

corrosion of various solutions were statistically analyzed, as shown in Table 3 (taking pH = 2 and pH = 7 as examples). The relationship between crushing energy consumption and impact velocity in three cases was fitted, respectively, and part of the results is shown in Figure 15. In order to distinguish it from the crushing energy consumption in the impact compression test, W_a is used to represent the crushing energy consumption in the dynamic point load test.

According to Figure 15, the relationship between the impact velocity and crushing energy consumption of corroded samples at different pH values during dynamic point load test was fitted. The fitting results are as follows: After

Table 2: Statistical table of test data on impact compression of samples after corrosion of pH = 2 and pH = 5 solutions.

Sample number	pH	V (m·s^{-1})	σ (MPa)	W (J)
1	2	9.97	117.44	36.66
2	2	10.76	132.33	46.33
3	2	11.57	149.69	52.69
4	2	11.85	162.33	60.17
5	2	12.74	171.14	66.32
6	2	13.01	210.17	74.31
7	5	9.77	118.32	40.84
8	5	10.22	130.54	43.87
9	5	10.78	147.36	50.02
10	5	11.23	160.11	54.73
11	5	12.74	184.26	70.69
12	5	13.41	227.66	82.63

pH = 2 solution corrosion, the fitting relationship is W_a = 15.523v–78.274 and coefficient of determination R^2 is 0.99, indicating a good degree of fitting. After pH = 5 solution corrosion, the fitting relation is W_a = 14.404v–70.972, coefficient of determination R^2 is 0.98, and the fitting degree is good. When pH = 7 solution corroded, the fitting relation was W_a = 14.042v–61.73 and the coefficient of determination R^2 was 0.99, indicating a good degree of fitting.

Combined with the fitting relationship between crushing energy consumption and the impact velocity in the impact compression test mentioned above, we can obtain the conversion relationship between crushing energy consumption W_1 in the impact compression test and crushing energy consumption W_a in the dynamic point load test at the same impact velocity after corrosion with different solutions, as shown in Figure 16. The conversion relationship formula is as follows: After corrosion with pH = 2 solution, the conversion relationship is W_1 = 0.753W_a–17.026; when

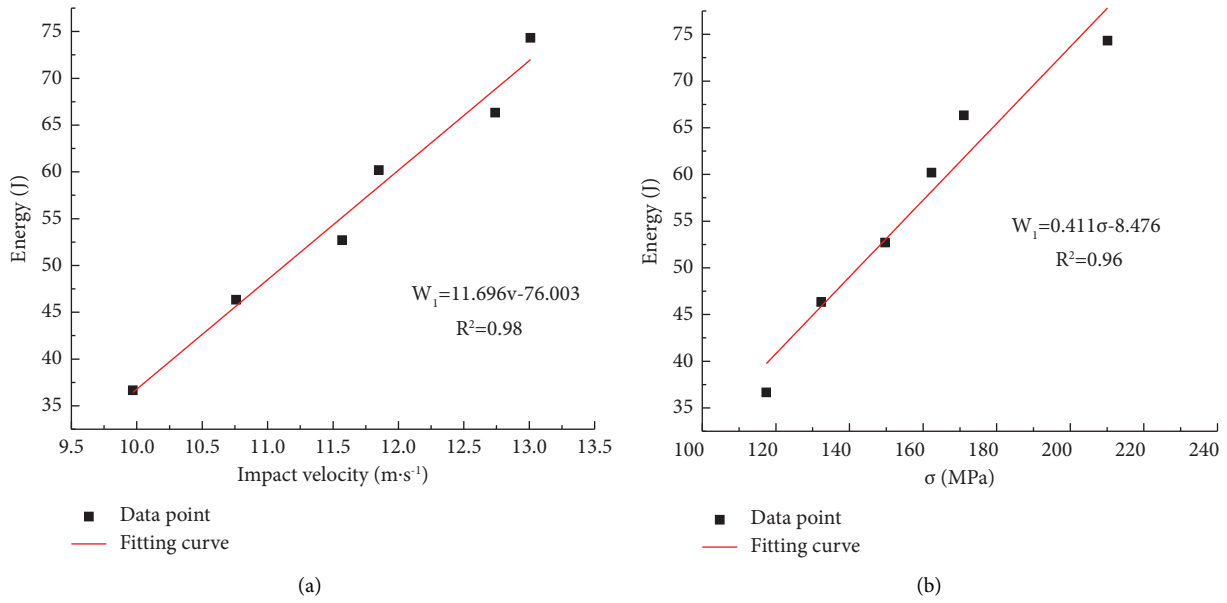

Figure 10: The fitting relationship between crushing energy consumption and impact velocity and dynamic compressive strength in the impact compression experiment of pH = 2 solution after corrosion: (a) impact velocity-crushing energy consumption fitting curve and (b) dynamic compressive strength-crushing energy consumption fitting curve.

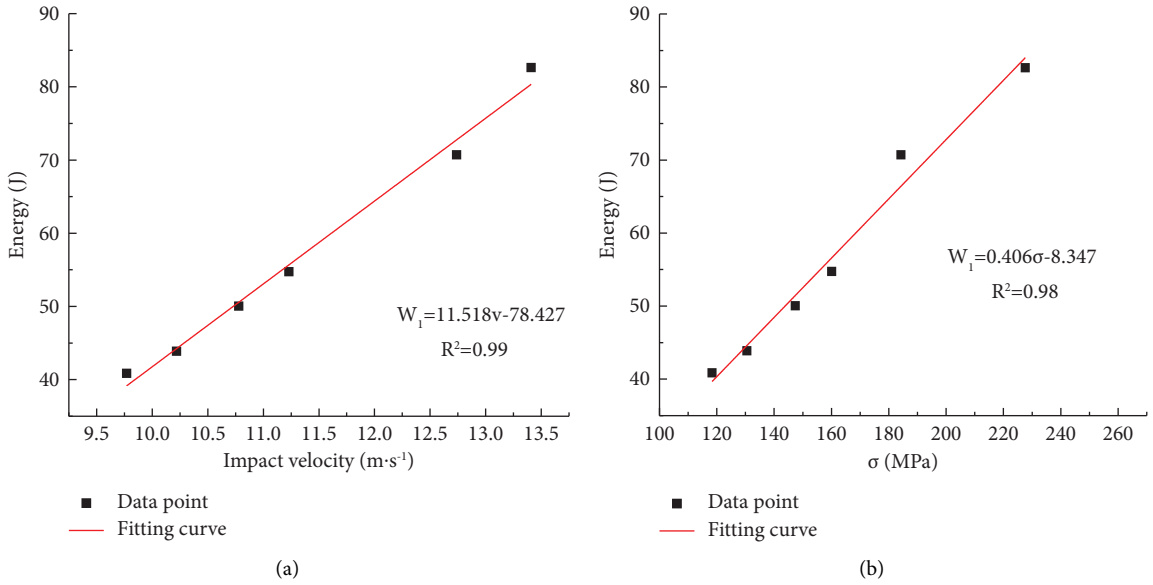

Figure 11: The fitting relationship between crushing energy consumption and impact velocity and dynamic compressive strength in the impact compression experiment of PH = 5 solution after corrosion: (a) impact velocity-crushing energy consumption fitting curve and (b) dynamic compressive strength-crushing energy consumption fitting curve.

pH = 5 solution is corroded, the conversion relationship is $W_1 = 0.761W_a - 17.386$; pH = 7. After the solution is corroded, the conversion relationship is $W_1 = 0.800W_a - 21.675$. The fitting relation between the above and the dynamic compressive strength is substituted into the corresponding fitting formula, respectively, and the conversion relation is $\sigma = 1.832W_a - 20.804$ after pH = 2 solution corrosion; pH = 5 solution corrosion, the conversion relationship is $\sigma = 1.971W_a - 32.827$; pH = 7. After solution corrosion, the conversion relationship is $\sigma = 2.204W_a - 47.184$.

The fitting curve between the three groups of dynamic compressive strength and the crushing energy consumption of the corresponding dynamic point load test is drawn in Figure 16. It can be seen that as the pH value of the corrosion solution decreases (the corrosion degree increases), the slope of the fitting relationship between the dynamic compressive strength and the crushing energy consumption in the dynamic point load test decreases. The three curves intersect when the crushing energy consumption in the dynamic point load test is about 70 J. In other words, when the

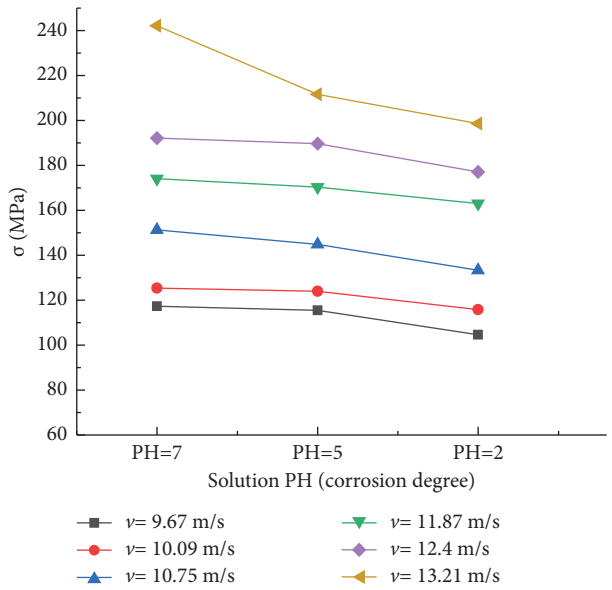

Figure 12: Dynamic compressive stress-strain curves of rocks corroded with pH = 7 solution at different impact velocities.

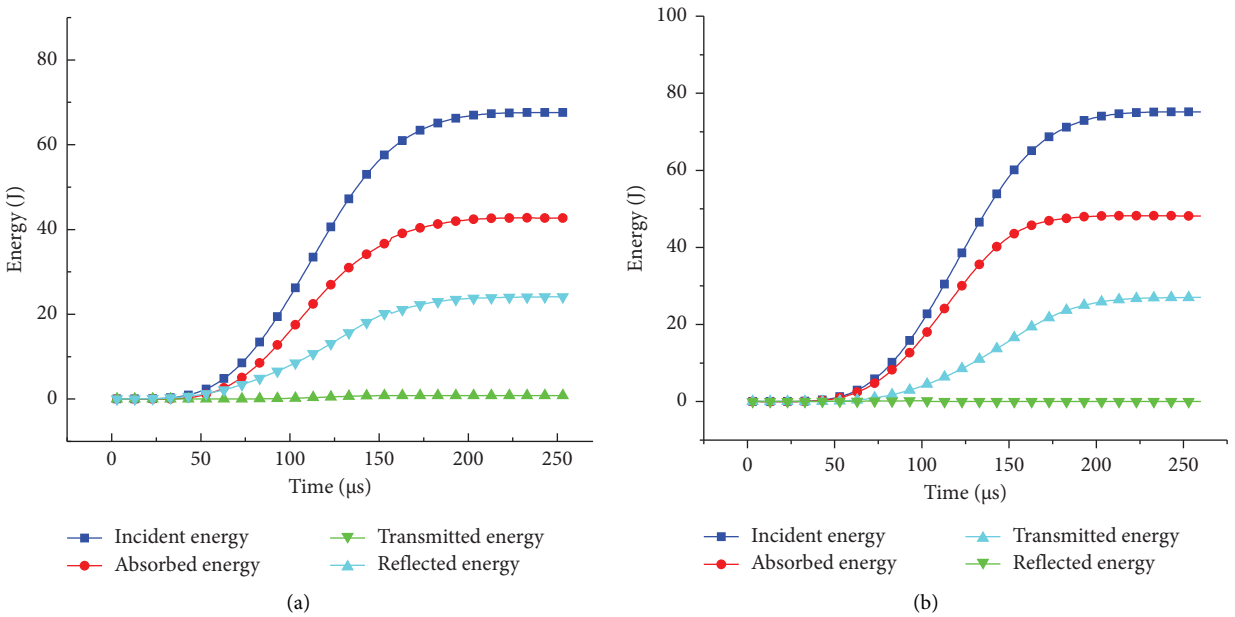

Figure 13: Continued.

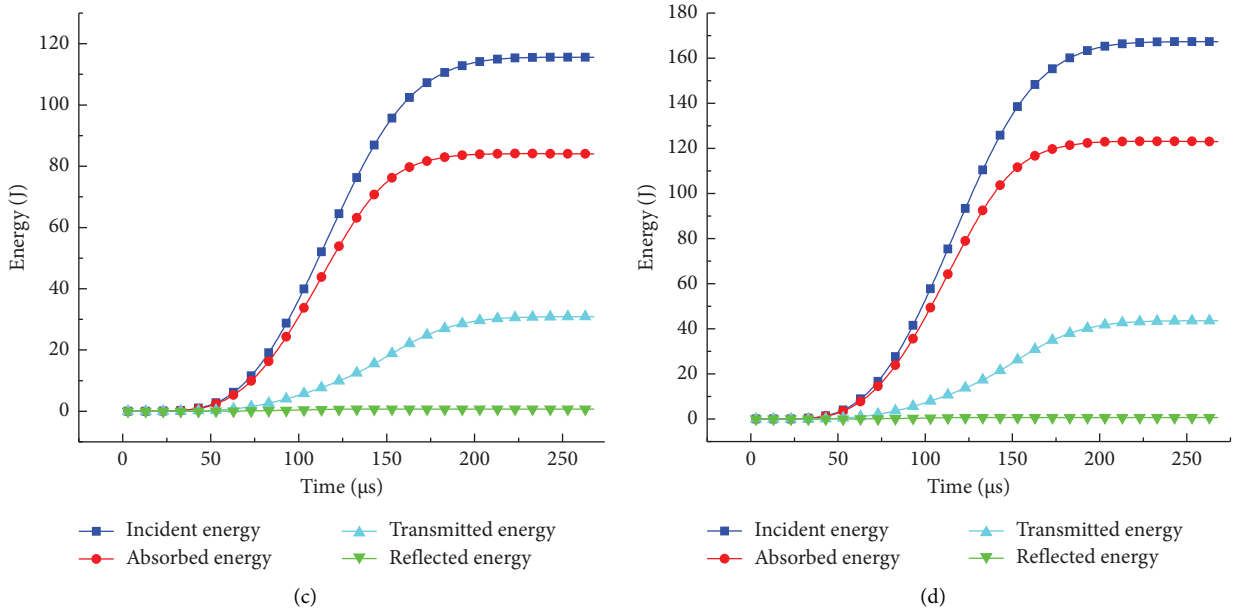

Figure 13: The energy time history of part of the impact compression test of the sample corroded by the solution with pH = 2: (a) impact velocity of 7.79 m/s, (b) impact velocity of 8.26 m/s, (c) impact velocity of 10.33 m/s, and (d) impact velocity of 13.01 m/s.

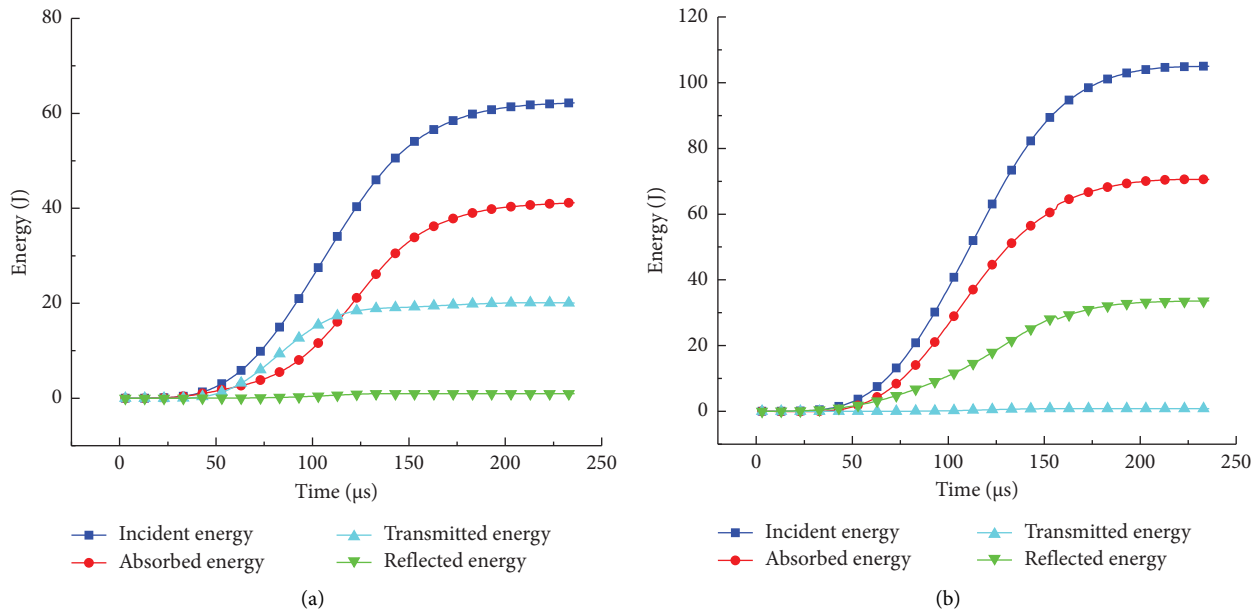

Figure 14: Continued.

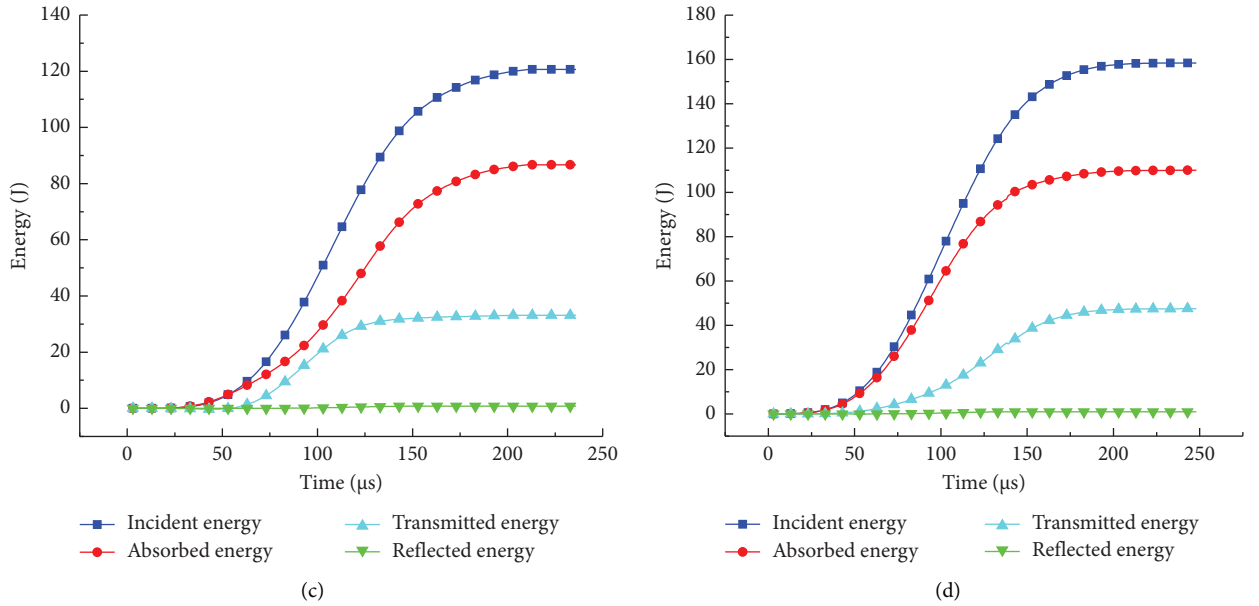

Figure 14: The energy time history of part of the impact compression test of the sample corroded by the solution with pH = 2: (a) impact velocity of 7.31 m/s, (b) impact velocity of 9.44 m/s, (c) impact velocity of 10.46 m/s, and (d) impact velocity of 12.22 m/s.

Table 3: Statistical table of dynamic point load test data of samples corroded by salt solution with pH = 2 and pH = 7.

Sample number	pH	V (m·s^{-1})	σ (MPa)	W_a (J)
1	2	6.59	46.79	24.62
2	2	7.79	67.33	42.02
3	2	8.26	74.76	48.75
4	2	10.33	115.23	84.02
5	2	10.79	126.32	89.22
6	2	13.01	167.29	122.99
7	7	7.31	62.01	41.02
8	7	8.35	82.01	54.98
9	7	9.44	105.31	70.51
10	7	10.46	120.66	86.73
11	7	11.87	149.68	104.02
12	7	12.22	158.41	109.96

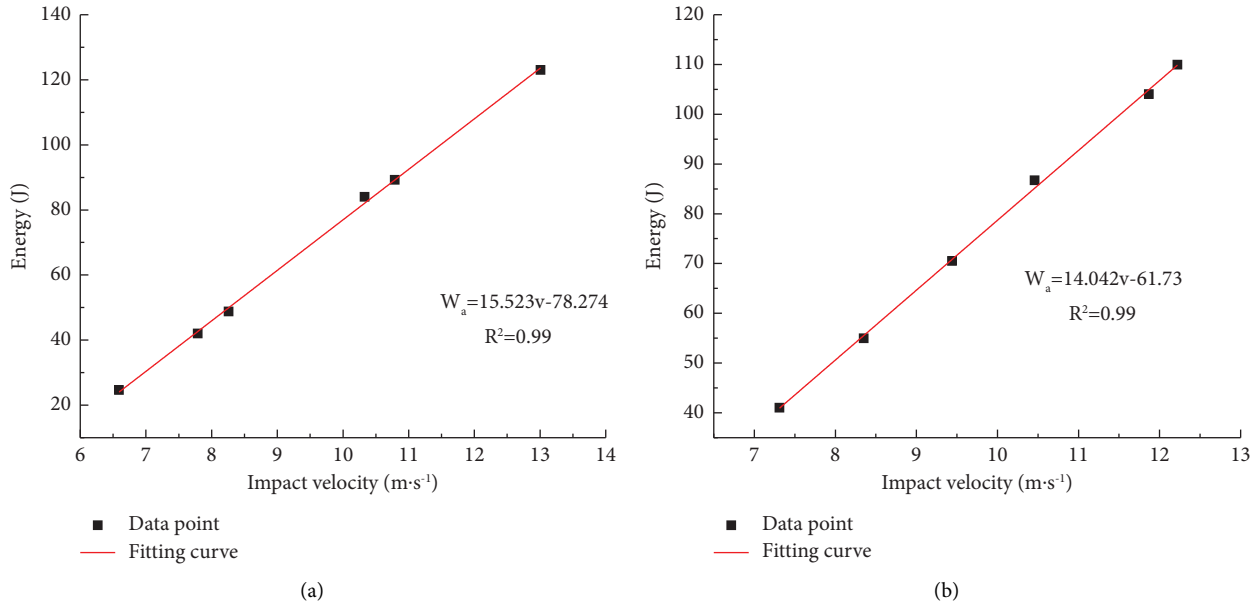

Figure 15: Fitting relationship between crushing energy consumption and impact velocity in dynamic point load test after corrosion with different solutions: (a) pH = 2 and (b) pH = 7.

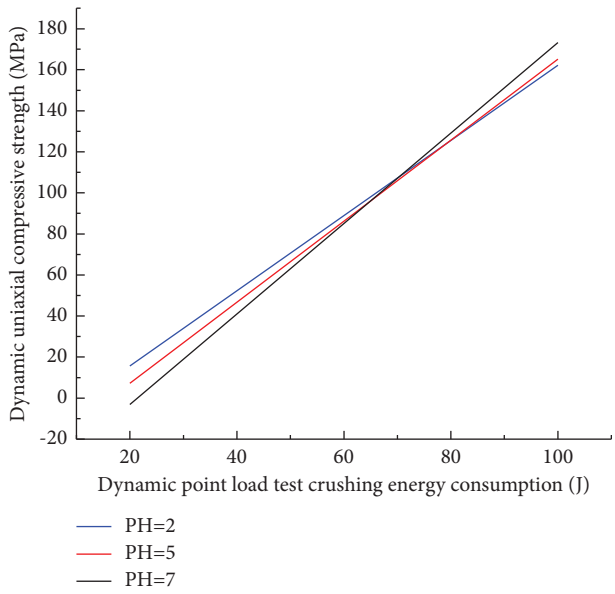

Figure 16: The relationship between crushing energy consumption and dynamic compressive strength in dynamic point load test after corrosion of different solutions.

crushing energy consumption in the dynamic point load test is used to estimate the dynamic compressive strength, a certain crushing energy consumption (the final value of this test is 70 J in this paper) is more accurate, and it can estimate the dynamic compressive strength under various corrosion conditions under this crushing energy consumption. However, with the change of crushing energy consumption in dynamic point load test, this transformation relationship is no longer accurate, and it is necessary to modify this transformation relationship with corrosion condition as the influence factor.

4. Conclusions and Future Work

The research results are as follows:

(i) The *P*-wave velocity of all samples decreased after corrosion of different pH solutions. If linear fitting is adopted, the *P*-wave velocity decline slopes of the corroded samples with pH values of 2, 5, and 7 are −11.65, −8.78, and −2.07, respectively; that is, the lower the pH value, the faster the wave velocity declines and the greater the final change range. At the same time, the change rate of wave velocity is large in the initial stage of the experiment and tends to be gentle in the later stage

(ii) The fitting relationship between the crushing energy consumption of dynamic compression test and dynamic point load test at the same impact speed is as follows: after corrosion by pH = 2 solution, the fitting relationship is $W_1 = 0.753W_a - 17.026$; after corrosion by pH = 5 solution, the fitting relation is $W_1 = 0.761W_a - 17.386$; and after corrosion by pH = 7 solution, the fitting relation is $W_1 = 0.800W_a - 21.675$

(iii) The fitting relationship between crushing energy consumption and dynamic compressive strength during the dynamic point load test after corrosion by salt solution with different pH values is as follows: After corrosion by solution with pH = 2, the fitting relationship is $\sigma = 1.832W_a - 20.804$; after pH = 5 solution corrosion, the fitting relation is $\sigma = 1.971W_a - 32.827$; and after pH = 7 solution corrosion, the fitting relation is $\sigma = 2.204W_a - 47.184$. This conclusion can provide reference for obtaining the dynamic compressive strength of rocks under different corrosion conditions in engineering field in the future

(iv) When the crushing energy consumption in the dynamic point load test is used to estimate the dynamic compressive strength, a certain crushing energy consumption (the final value of this test is 70 J in this paper) is more accurate, and it can estimate the dynamic compressive strength under various corrosion conditions under this crushing energy consumption. However, with the change of crushing energy consumption in the dynamic point load test, this transformation relationship is no longer accurate, and it is necessary to modify this transformation relationship with corrosion condition as the influence factor.

However, due to the limited amount of experimental data, further work will include the following two points:

(1) In static point load test, the Committee of the International Society for Rock Mechanics recommended the use of the rock point load strength test method in 1972, and in 1985, it proposed a revised method to calculate the uniaxial compressive strength of rock, which has been widely recognized by most scholars [27]. In this paper, only one kind of rock, granite, is discussed, and whether the obtained law can be as universal as in the static case needs to be verified by a large number of experiments in the later stage.

(2) In the static point load test, the point load strength can be used to determine the compressive strength and tensile strength of rock. However, this paper only establishes the relationship between the dynamic point load strength and the dynamic compressive strength. The relationship between dynamic tensile strength and dynamic point load strength needs to be further verified by the dynamic splitting test in the later stage.

Data Availability

Some or all data, models, or codes generated or used during the study are proprietary or confidential in nature and may only be provided with restrictions.

Conflicts of Interest

The authors declare that they have no conflicts of interest.

Acknowledgments

This research was funded by the National Natural Science Foundation of China (52274107 and 52374113), the Excellent Youth Team Project for the Central Universities (FRF-EYIT-23-01), and the Beijing Nova Program (20230484242).

References

[1] J. Lu, G. Z. Yin, D. M. Zhang, H. Gao, C. B. Li, and M. H. Li, "True triaxial strength and failure characteristics of cubic coal and sandstone under different loading paths," *International Journal of Rock Mechanics and Mining Sciences*, vol. 135, Article ID 104439, 15 pages, 2020.

[2] S. L. Quane and J. K. Russell, "Rock strength as a metric of welding intensity in pyroclastic deposits," *European Journal of Mineralogy*, vol. 15, no. 5, pp. 855–864, 2003.

[3] R. H. C. Wong, K. T. Chau, J. H. Yin, D. T. W. Lai, and G. S. Zhao, "Uniaxial compressive strength and point load index of volcanic irregular lumps," *International Journal of Rock Mechanics and Mining Sciences*, vol. 93, pp. 307–315, 2017.

[4] D. K. Ghosh and M. Srivastava, "Point-load strength: an index for classification of rock material," *Bulletin of the International Association of Engineering Geology*, vol. 44, no. 1, pp. 27–33, 1991.

[5] D. Li and L. N. Y. Wong, "Point load test on meta-sedimentary rocks and correlation to UCS and BTS," *Rock Mechanics and Rock Engineering*, vol. 46, no. 4, pp. 889–896, 2013.

[6] Y. Shao, C. H. Yan, and Q. H. Ma, "Correlation analysis of dayangshan rock strength in suzhou," *Journal of Yangtze River Scientific Research Institute*, vol. 32, no. 10, pp. 107–110, 2015.

[7] M. Koohmishi and M. Palassi, "Evaluation of the strength of railway ballast using point load test for various size fractions and particle shapes," *Rock Mechanics and Rock Engineering*, vol. 49, no. 7, pp. 2655–2664, 2016.

[8] J. K. Li, F. F. Li, and X. K. Wei, "The effect of specimen's height on the point load test," *Advanced Materials Research*, vol. 848, pp. 108–111, 2013.

[9] J. H. Yin, R. H. C. Wong, K. T. Chau, D. T. W. Lai, and G. S. Zhao, "Point load strength index of granitic irregular lumps: size correction and correlation with uniaxial compressive strength," *Tunnelling and Underground Space Technology*, vol. 70, pp. 388–399, 2017.

[10] N. Turk and W. R. Dearman, "Improvements in the determination of point load strength," *Bulletin of the International Association of Engineering Geology*, vol. 31, no. 1, pp. 137–142, 1985.

[11] Y. P. Wang, Y. H. Wang, Z. H. Zhao, and J. M. Ma, "Analysis of the rock stiffness in the point load test for rock mass classification in mining engineering," *Journal of Hefei University of Technology*, vol. 30, no. 10, pp. 1353–1356, 2007.

[12] M. Zhou, L. Qiao, Q. W. Li, S. Yang, and Z. Huang, "Research on the conversion relationship between dynamic point load strength and dynamic compressive strength based on energy system," *Shock and Vibration*, vol. 2022, Article ID 6988292, 10 pages, 2022.

[13] Y. S. Liu, W. Liu, and X. Y. Dong, "Dynamic mechanical properties and constitutive model of rock under chemical corrosion," *Journal of Yangtze River Scientific Research Institute*, vol. 32, no. 5, pp. 72–75, 2015.

[14] Y. Lin, K. P. Zhou, F. Gao, and J. L. Li, "Damage evolution behavior and constitutive model of sandstone subjected to chemical corrosion," *Bulletin of Engineering Geology and the Environment*, vol. 78, no. 8, pp. 5991–6002, 2019.

[15] J. C. Xue, Z. Y. Zhao, L. J. Dong et al., "Effect of chemical corrosion and axial compression on the dynamic strength degradation characteristics of white sandstone under cyclic impact," *Minerals*, vol. 12, no. 4, p. 12, 2022.

[16] W. X. Ding, X. T. Feng, and B. R. Chen, "Study on the mechanical property and the evolutionary neural network constitutive model for limestone under chemical corrosive environments," *Key Engineering Materials*, vol. 340-341, pp. 1169–1174, 2007.

[17] W. Wang, T. G. Liu, X. H. Li, R. B. Wang, and W. Y. Xu, "Mechanical behaviour of granite in triaxial compression under chemical corrosion," *Journal of Central South University of Science and Technology*, vol. 46, no. 10, pp. 3801–3807, 2015.

[18] S. J. Miao, M. F. Cai, D. Ji, and Y. B. Bai, "Aging features and mechanism of Granite's damage under the action ofacidic chemical solutions," *Journal of China Coal Society*, vol. 41, no. 5, pp. 1137–1144, 2016.

[19] Y. C. Yin, Y. L. Chen, and X. R. Meng, "Comparison of mechanical properties and fracture toughness changes of sandstone and granite under freeze-thaw cycle and chemical corrosion," *Journal of Water Resources and Water Engineering*, vol. 30, no. 4, pp. 217–224, 2019.

[20] M. G. Karfakis and M. Akram, "Effects of chemical solutions on rock fracturing," *International Journal of Rock Mechanics and Mining Sciences & Geomechanics Abstracts*, vol. 30, no. 7, pp. 1253–1259, 1993.

[21] T. Heggheim, M. V. Madland, R. Risnes, and T. Austad, "A chemical induced enhanced weakening of chalk by seawater," *Journal of Petroleum Science and Engineering*, vol. 46, no. 3, pp. 171–184, 2005.

[22] J. Sausse, E. Jacquot, B. Fritz, J. Leroy, and M. Lespinasse, "Evolution of crack permeability during fluid–rock interaction. Example of the Brezouard granite (Vosges, France)," *Tectonophysics*, vol. 336, no. 1-4, pp. 199–214, 2001.

[23] K. Su, N. Hoteit, and O. Ozanam, "Evolution of crack permeability during fluid–rock interaction. Example of the Brezouard granite (Vosges, France)," *Elsevier Geo-Engineering Book Series*, pp. 419–424, Elsevier, Amsterdam, Netherlands, 2004.

[24] A. Polak, D. Elsworth, J. Liu, and A. S. Grader, "Spontaneous switching of permeability changes in a limestone fracture with net dissolution," *Water Resources Research*, vol. 40, no. 3, p. 10, 2004.

[25] H. Yasuhara, A. Polak, Y. Mitani, A. S. Grader, P. M. Halleck, and D. Elsworth, "Evolution of fracture permeability through fluid-rock reaction under hydrothermal conditions," *Earth and Planetary Science Letters*, vol. 244, no. 1-2, pp. 186–200, 2006.

[26] J. S. Liu, J. C. Sheng, A. Polak, D. Elsworth, H. Yasuhara, and A. S. Grader, "A fully-coupled hydrological–mechanical–chemical model for fracture sealing and preferential opening," *International Journal of Rock Mechanics and Mining Sciences*, vol. 43, no. 1, pp. 23–36, 2006.

[27] J. A. Franklin, "Suggested method for determining point load strength," *International Journal of Rock Mechanics and Mining Sciences and Geomechanics Abstracts*, vol. 22, no. 2, pp. 51–60, 1985.